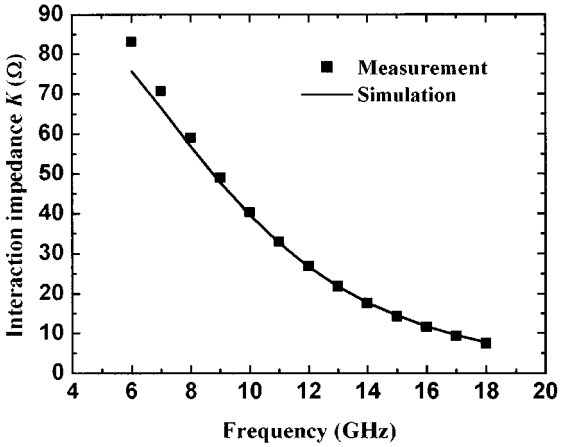

Fig. 4. Comparison of measured (by a nonresonant perturbation method using a very thin conductive wire with 20-μm diameter) and calculated (by an HFSS code) interaction impedance for the helical SWS.

The measurement with the perturber of the smallest size of 20 μm provides the best agreement with the simulation, as shown in Fig. 4. The largest discrepancy is within 10% at the lowest frequency and within 5% at the highest frequency. This discrepancy is noticeably less than that found by measurements using a dielectric perturber [3]. It seems it is the best agreement between the simulation and measurement reported for the helix interaction impedance.

IV. Conclusions

In this paper, the effects of the conductive wire on the measurement accuracy of the interaction impedance have been carried out by the nonresonant perturbation method varying the diameter of the wire. When the conductive wire diameter is approximately 2% of the helix diameter, the discrepancy between the measured and simulated values become small enough to be used for the reciprocal evaluation of software and measurement that may be helpful in TWT design. The measured values of the interaction impedance converge to the simulated ones when the wire diameter is reduced to less than 10% of the helix diameter. Therefore, the measurement method using a hairline conductive wire as a perturber is superior to the commonly used methods using a dielectric rod.

Acknowledgment

The authors would like to thank Dr. J. A. Dayton, Jr., Boeing and Dr. C. L. Kory for the careful reading of this paper's manuscript and for useful comments. Dr. H. S. Kim and J. H. Lee, KMW Inc., Hwa Sung City, Korea, are also acknowledged for their assistance with supplying microwave components.

References

[1] J. R. Pierce, *Traveling-Wave Tubes*. New York: Van Nostrand, 1950.
[2] R. P. Lagerstrom, "Interaction impedance measurement by perturbation of traveling waves," Stanford Electron. Lab., Stanford Univ., Stanford, CA, Tech. Rep. 7, Feb. 1957.
[3] C. L. Kory and J. A. Dayton, Jr., "Computational investigation of experimental interaction impedance obtained by perturbation for helical traveling-wave tube structures," *IEEE Trans. Electron Devices*, vol. 45, pp. 2063–2071, Sept. 1998.
[4] P. Wang, R. Carter, and B. N. Basu, "An improved technique for measuring the Pierce impedance of helix slow-wave structures," in *Proc. Eur. Microwave Conf.*, 1994, pp. 25–30.
[5] S. J. Rao, S. Ghosh, P. K. Jain, and B. N. Basu, "Nonresonant perturbation measurements on dispersion and interaction impedance characteristics of helical slow-wave structures," *IEEE Trans. Microwave Theory Tech.*, vol. 45, pp. 1585–1593, Sept. 1997.
[6] *HFSS 7.0 User's Electronic Manual*, Ansoft Corporation, Pittsburgh, PA, 1999.
[7] A. V. Soukhov, S.-S. Jung, and G.-S. Park, "Diffraction model for an interaction impedance measurement using nonresonant method," *J. Korean Phys. Soc.*, vol. 38, no. 6, pp. 762–765, June 2001.
[8] J. R. Legarra, "Measurement of microwave characteristics of helix traveling wave circuits," in *IEEE Int. Electron Devices Meeting Tech. Dig.*, Dec. 1979, pp. 401–411.
[9] C. L. Kory and J. A. Dayton, Jr., "Effect of helical slow-wave circuit variations on TWT cold-test characteristics," *IEEE Trans. Electron Devices*, vol. 45, pp. 972–976, Apr. 1998.

A 7.5-GHz Super Regenerative Detector

N. B. Buchanan, V. F. Fusco, and J. A. C. Stewart

***Abstract*—In this paper, simulated and measured results are presented for a microwave-integrated-circuit super regenerative detector operating at 7.5 GHz and brief comparisons made to a monolithic-microwave integrated-circuit super regenerative detector operating at 34 GHz. The sensitivity of the 7.5-GHz detector was measured at −83-dBm (AM, 1 kHz, 100% mod) RF signal for 12 dB (signal + noise + distortion)/(noise + distortion). Simulation results show that, to produce a sensitive super regenerative detector, a high rate of change in loop gain of the oscillator circuit with respect to the gate bias (quenching) voltage and a high maximum loop gain at the point of detection is required. It has also been shown, by simulation and measurement, that the detection frequency of the super regenerative detector is lower than the normal free-running oscillation frequency.**

***Index Terms*—Microwave detectors, microwave oscillators, microwave receivers, super regenerative detectors.**

I. Introduction

The super regenerative detector operates on the direct conversion principle where a circuit consisting of as little as one active device can perform RF detection and demodulation, allowing the possibility of a low component-count microwave receiver. In comparison, the more commonly used super heterodyne detector operates by mixing the RF signal down to a lower intermediate frequency for demodulation. This improves performance at the expense of a higher component count, which may be undesirable at millimeter-wave frequencies.

Theoretical explanations for super regenerative detectors have been described in [1]–[3] and, more recently, simulation methods have been presented in [4]. In this paper, simulated and measured results are presented for a microwave-integrated-circuit (MIC) detector operating at 7.5 GHz and brief comparisons made to a previously reported (The Queens University of Belfast (QUB), Belfast, Northern Ireland) [5] super regenerative monolithic-microwave integrated-circuit (MMIC) detector operating at 34 GHz.

The super regenerative detector described here operates by applying a signal to the gate bias connection of an oscillator at a rate called the

Manuscript received June 11, 2001.

The authors are with the Department of Electrical and Electronic Engineering, The Queens University of Belfast, Belfast BT9 5AH, Northern Ireland (e-mail: n.buchanan@ee.qub.ac.uk).

Publisher Item Identifier 10.1109/TMTT.2002.802336.

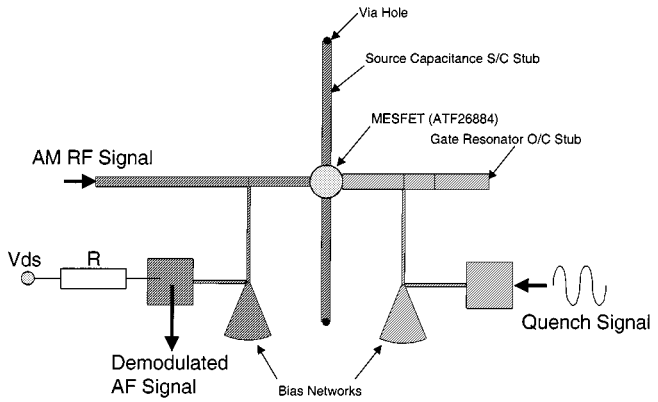

Fig. 1. Layout of 7.5-GHz MIC oscillator circuit.

quench frequency. This has the effect of bringing the circuit rapidly in and out of oscillation. Detection occurs when an amplitude modulated signal is applied to the circuit, the demodulated signal being recovered from the drain current. A quenching frequency at least several times higher than the modulating frequency of the RF signal must be used for satisfactory detection to take place. It has been previously shown in [1]–[3] that the high amplification of the super regenerative detector occurs at the point on the quench waveform when the oscillator is just beginning to oscillate.

This type of sensor has applications in short-haul communication links where a simple low-cost detector is required.

II. Super Regenerative Detector Design Methods

The small-signal open-loop gain or HP-MDS[1] Oscport method was used in HP-MDS to determine the start-up conditions for the 7.5-GHz oscillator to be deployed as a super regenerative detector. The circuit of Fig. 1 was simulated to obtain values of open loop gain for the oscillator. A gate bias point of $V_{\rm GS} = -0.4$ V was chosen, which gave a value of $I_{\rm DS} = 20$ mA with $V_{\rm DS} = 5.0$ V, Fig. 2(a) indicates a loop gain of 10 dB when the phase of the loop gain is zero. This result indicates that the circuit may oscillate at this frequency point (8.36 GHz). The oscillation start up is then confirmed by studying the Nyquist plot of Fig. 2(b). This shows that the loop gain of the circuit encircles the $[+1, j0]$ point in a clockwise direction, indicating that oscillation will occur [7].

III. Measurement Setup

In order to measure the oscillator in a super regenerative detector configuration, the setup of Fig. 3 was used. When the detector was measured, the amplitude-modulated RF signal was coupled to the output port by means of a directional coupler. The demodulated signal was detected by tapping off the drain current, which was observed across the resistance R; a value of 100 Ω being used in this case. This signal was fed either into an oscilloscope or a Radio Communications Test Set, which enabled the received signal (signal + noise + distortion)/(noise + distortion) (SINAD) to be measured.

A. Initial Measurements

The circuit was initially quenched at a frequency of 1 MHz, using a sine-wave signal. The amplitude and dc offset of the quench waveform were varied until the characteristic "noise" of the detector was observed on the audio output of the radio communications test set. A

[1]*HP Microwave RF Des. Syst.*, rel. 7.0, Hewlett-Packard Company, Santa Rosa, CA, 1997.

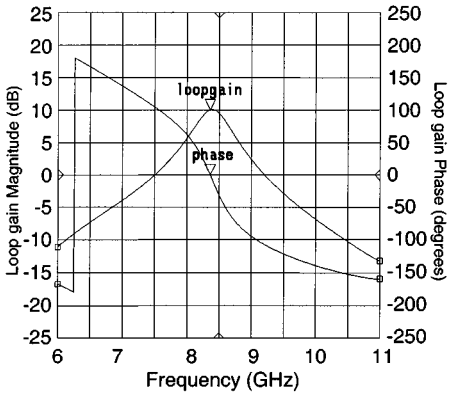

(a)

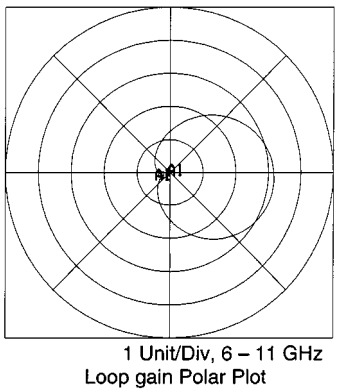

(b)

Fig. 2. Simulation results of Oscport analysis.

stable operating point was found where the characteristic noise was present without requiring overcritical quench adjustments.

The characteristic quenching noise was found to be present when the amplitude of the quench signal was increased to 1.1 V p-p with no dc offset present. Application of a −81.5-dBm (AM, 1 kHz, 100% mod) RF signal produced 12-dB SINAD, indicating good sensitivity. The RF was swept to find the most sensitive input signal frequency, i.e., in this case, 7.47 GHz. The "noise" was also present when a negative dc offset was applied to a 1-V p-p quench signal, although this operating point was quickly ruled out as the application of an RF signal to the detector showed very poor sensitivity.

It was noticed that the optimum detection frequency (7.47 GHz) was significantly lower than the simulated free-running oscillation frequency of 8.36 GHz. Here it was suspected that a frequency-pushing effect was occurring, causing the device frequency to vary with the gate bias.

B. Effect of Quenching Conditions on Detector Operation

Varying the quench frequency to 600 kHz produced optimum sensitivity at −83 dBm (AM, 1 kHz, 100% mod) for a 12-dB SINAD. Quenching using a triangular waveform degraded the sensitivity by approximately 2 dB, while a square wave quench caused considerable distortion; although this effect was to be expected from the discussions in [2] and [3].

The applied RF signal level required to maintain a 12-dB SINAD is shown in Fig. 4 as a function of quench frequency. These results show that a broad optimum quench frequency band exists for this circuit.

C. Spectral Analysis to Determine Frequency-Pushing Effects

One well-known disadvantage of a super regenerative detector is the radiation of unwanted signals. This is to be expected since the detector

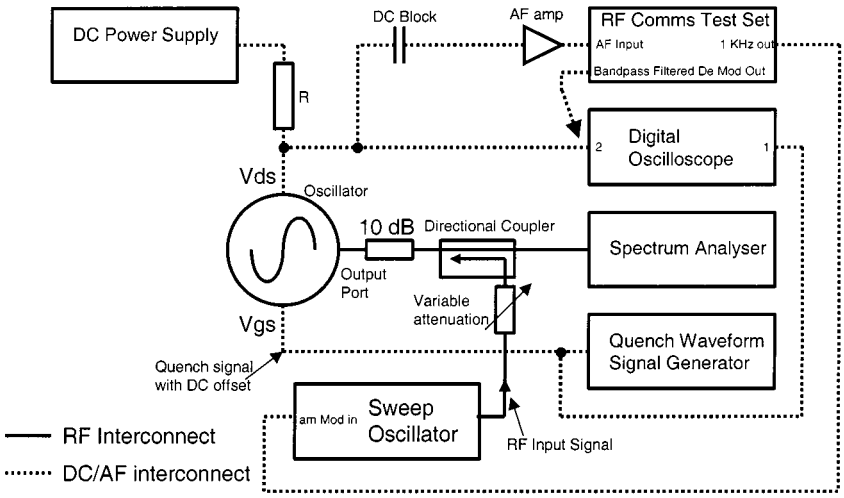

Fig. 3. Measurement setup for 7.5-GHz MIC super regenerative detector.

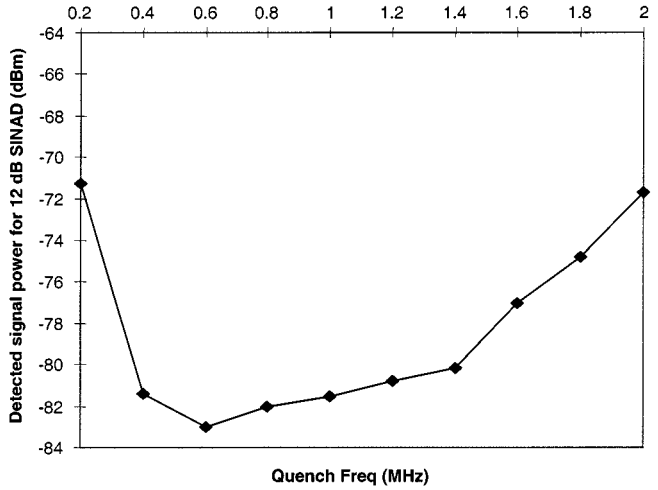

Fig. 4. Signal level required for 12-dB SINAD over various quench frequencies.

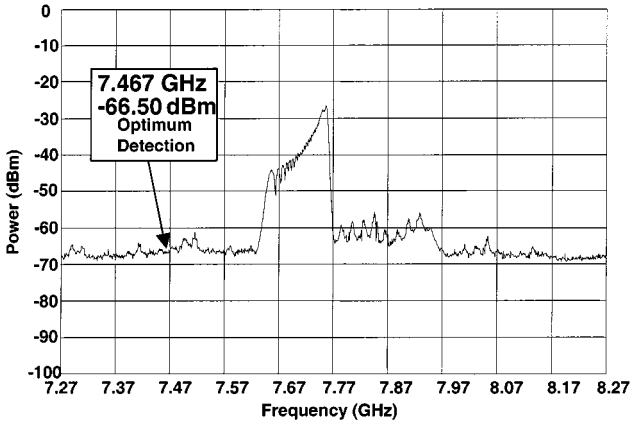

Fig. 5. RF spectrum of 7.5-GHz MIC super regenerative detector.

is a quasi-oscillating circuit. Also, according to the theory of [3], when the oscillation is occurring at full amplitude, no detection takes place, making the output an unwanted by-product. The detectors observed by [1]–[3] used vacuum tube devices and detection was observed to occur at the oscillation frequency, i.e., no bias frequency pushing. The spectrum at the output of the detector was examined in order to determine what additional effects occur in a detector employing a MESFET device, i.e., with potential bias pushing.

The plot of Fig. 5 shows the output spectrum of the detector when it is working at optimum sensitivity. Here, it is observed that the frequency of the detector varies by 0.11 GHz, indicating the circuit's frequency is being pushed by the gate bias (quench) voltage. This phenomenon operated as follows. Varying the gate bias of this type of oscillator [6] produces a frequency-pushing effect via the nonlinear device gate–source voltage-dependant capacitance. This causes the frequency of the oscillator to vary by means of the quenching signal. The frequency at which optimum detection sensitivity occurred is shown in Fig. 5. It was observed from this that the detection does not take place at the normal free-running oscillator frequency, but at one approximately 0.3 GHz lower, due to the dynamic frequency-pushing effect from the quench signal.

D. Comparison Between Static and Dynamic Frequency-Pushing Characteristics

Since the MIC super regenerative detector operated at around 7.5 GHz, some of the types of measurements that have been made on lower frequency detectors could not be repeated here. One of the most notable of these was the inability to examine the time-domain signal on an oscilloscope; consequently, in this section, the frequency-pushing characteristics of the oscillator operating under a fixed dc quench voltage (static) were measured and compared with the dynamic characteristic. From this measurement, an approximate model of the detection process may be produced.

The static characteristics of the detector are plotted in Fig. 6. The arrows on the plot indicate that the measurement was carried out by increasing the dc quench voltage. At the beginning of the measurement (dc quench $= -0.65$ V) the circuit was oscillating at a frequency of 7.758 GHz. It continued to oscillate until the dc quench voltage reached -0.35 V where a frequency of 7.744 GHz was produced. When the oscillations ceased, a sudden change in the drain current caused the gate voltage to rise to 0.16 V; this voltage was then required to be reduced to -0.42 V for oscillation to recommence. The dotted-line portion of the graph indicates this nonoscillating state. These results showed a hysteresis effect on the static characteristics as the dc quench voltages required to stop and start the oscillation were different.

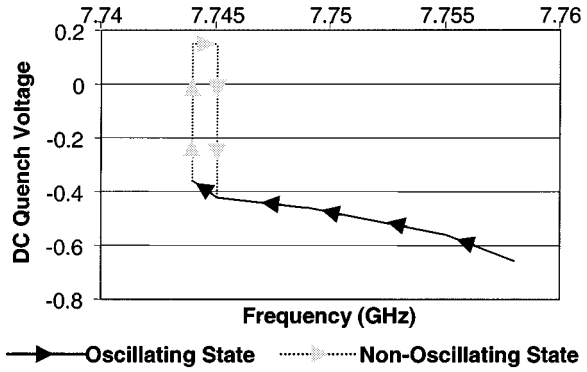

Fig. 6. Static quenching characteristics of 7.5-GHz super regenerative detector.

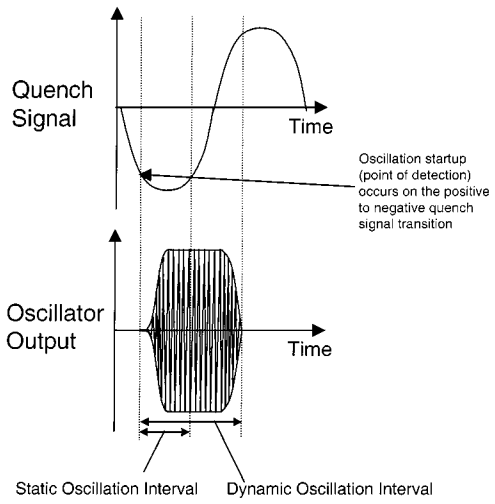

Fig. 7. Typical RF envelopes produced from quenching the 7.5-GHz MIC detector.

Observing the spectrum display of Fig. 5 indicates that the visible oscillations vary between 7.65–7.76 GHz, representing a frequency variation of 0.11 GHz for a 1.1-V p-p quench signal (0.1 GHz/V). Also, knowing that the optimum detection takes place 0.3 GHz below the maximum frequency of oscillation, the overall frequency-pushing range is likely to be larger than that observed from the spectrum display.

The static characteristics indicate a frequency variation of 0.014 GHz over a dc quench variation of 0.31 V (0.045 GHz/V). This indicates that the frequency range possible when the circuit is dynamically quenched is considerably higher than for the static case. The likely explanation for this is that, in the dynamically quenched case, the oscillations continue well into the positive region of the quench cycle since it takes a finite time for them to cease. The oscillations will again recommence when the quench voltage becomes sufficiently negative. A typical RF envelope that would be produced in this case is shown in Fig. 7. Here, the oscillations commence when the quench voltage is sufficiently negative. The resulting interval of oscillation is then shown to be higher for the dynamically quenched case due to the oscillations "running on" for a certain time period.

This analysis has shown that oscillator start up and, hence, detection, occurs on the positive-to-negative transition of the quench waveform. Traditionally, valve-based detectors have been shown [1]–[3] to detect on the negative-to-positive quench signal transition. Further simulations were carried out to the circuit in order to explain this behavior.

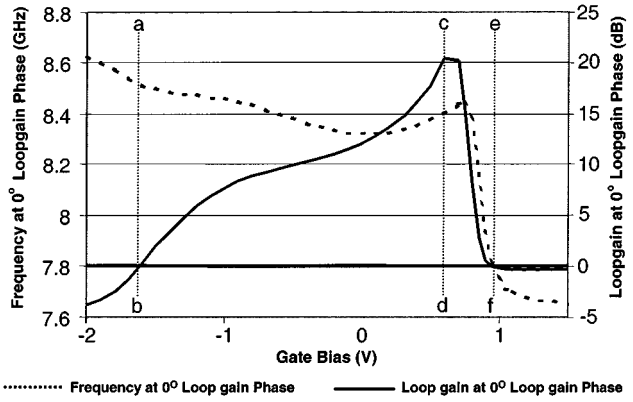

Fig. 8. Simulated frequency and loop gain at 0° loop-gain phase for 7.5-GHz MIC detector.

E. Quenching-Behavior Simulation

To confirm the quenching behavior of the MESFET oscillator, small-signal simulations were carried out on the circuit of Fig. 1 at various gate-bias voltages using HP-MDS. These produced loop-gain plots of a type similar to Fig. 2. At each bias point, the loop gain and frequency were noted when the loop-gain phase was 0°. This was the point where oscillation start up was likely to occur. These results are illustrated in the plot of Fig. 8. A significant frequency-pushing effect with gate bias is seen, with a frequency variation of 1 GHz being observed throughout the simulation range (dotted trace line of Fig. 8).

An interesting effect shown in Fig. 8 is the variation in loop gain with gate bias. The line *a–b* in Fig. 8 shows the loop gain at 0 dB, hence, no oscillation should occur. Moving to the right-hand side of this line (increasing gate bias), the line *c–d* is reached, indicating maximum loop gain. The loop gain then falls rapidly to the line *e–f*, where no oscillation should occur. It has been shown that the MIC detector detects when the oscillator starts up on the positive-to-negative quench signal transition. This relates to the period starting from line *e–f*, moving to maximum loop gain at line *c–d* in Fig. 8. It is noticed here that the loop gain rises considerably more rapidly between lines *e–f* to *c–d* ($\approx$ 70 dB/V), compared to the region lying between *a–b* to *c–d* ($\approx$ 10 dB/V). It was observed from practical results that quenching the circuit with a negative dc offset on the quench waveform produced poor sensitivity. In this case, the detector would have been operating along the line *a–b* to *c–d*, where a more gradual increase in loop gain was present.

The frequency variation observed during detection may also be observed from Fig. 8. Over the region *e–f* to *c–d*, where detection was assumed to occur, the frequency is seen to increase from 7.8 to 8.4 GHz. Detection is likely to take place at a point slightly to the left-hand side of line *e–f* since, here, the maximum rate of change of loop gain of 70 dB/V occurs. This is followed by oscillation at an increasing frequency as the loop gain rises. This explains why detection occurred at a frequency lower than the oscillation frequency, as observed in the spectrum display of Fig. 5.

A similar loop-gain analysis carried out to a 34-GHz MMIC super regenerative detector previously reported by QUB [5] showed that the most rapid rate of increase of the loop gain occurred on the negative-to-positive transition of the gate-bias voltage, opposite to that of the 7.5-GHz detector. These simulations were confirmed by measurement where both detectors were found to produce optimum performance under opposite quenching conditions.

The simulated rate of change of loop gain for the 34-GHz MMIC detector (15 dB/V) was observed to be less than that of the 7.5-GHz MIC (70 dB/V), also the maximum loop gain of the 34-GHz MMIC (2.25 dB) was significantly less than the 7.5-GHz MIC (20.5 dB). This

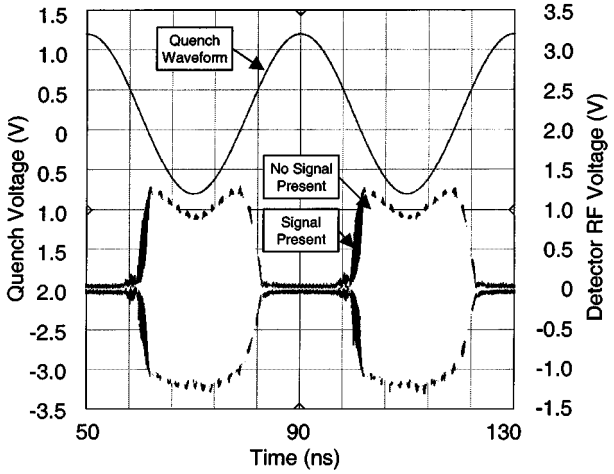

Fig. 9. 7.5-GHz MIC detector time-domain simulation.

provided an explanation as to why the 34-GHz MMIC detector reported in [5] was 22 dB less sensitive than the 7.5-GHz MIC. This also agrees with the theory of [3] since the MMIC has a lower loop gain; hence, less regeneration is present in the circuit, giving poorer sensitivity.

Therefore, to obtain a sensitive super regenerative detector, the quench voltage should be adjusted at a point where the rate of change of loop gain (or negative resistance) rises most rapidly at oscillator start up. This observation may also have design implications, as circuits could be designed specifically to possess a sharp rise in loop gain. Also, from the simulation results, it could be determined what type of quench waveform would be required for optimum sensitivity.

F. Time-Domain Analysis of RF Envelope

To determine the behavior of the super regenerative detector circuit under actual quenching conditions, a time-domain simulation using HP-MDS was carried out. To be able to simulate several quench cycles while maintaining the total number of time steps below CPU and memory restrictions, a sinusoidal quench frequency of 25 MHz was used instead of the measured 1-MHz range. Two simulations were carried out: one with no applied RF signal and another with a -40-dBm 8-GHz signal applied to the output port. The simulation result of Fig. 9 show that the oscillations are slightly advanced in the presence of an external RF signal, correlating with the findings of [1]–[3]. Another observation is that the oscillations show the effect of the dynamic quenching, as illustrated in Fig. 7. Fig. 9 shows the oscillations beginning to commence at a quench voltage of -0.3 V and not ceasing fully until the quench voltage has reached 0.6 V, indicating the oscillations to "run on" slightly when dynamically quenched.

IV. Conclusions

Results have been reported in this paper for a MIC detector operating at 7.5 GHz and comparisons made with a 34-GHz MMIC detector [5]. The 7.5-GHz detector was measured to detect a -83-dBm (AM, 1 kHz, 100% mod) RF signal for 12-dB SINAD compared to -61 dBm in the 34-GHz case. An optimum quenching frequency was found experimentally, which agreed with the findings of [2] and [3]. A spectrum display showed the detection frequency to be lower than the normal free-running frequency of the oscillator by typically 0.3 GHz. This was caused by the frequency-pushing effect of the quench signal applied to the gate of the active device, which was confirmed by small-signal loop-gain analysis.

Simulation of the loop gain and measured results of the 7.5- and 34-GHz super regenerative detectors has devised a design philosophy. Namely, the requirement for a sensitive detector to have a high rate of increase in loop gain and a high overall maximum loop gain at the point of detection.

References

[1] E. H. Armstrong, "Some recent developments of regenerative circuits," *Proc. Inst. Radio Eng.*, vol. 10, pp. 244–260, Aug. 1922.
[2] H. Ataka, "On superregeneration of an ultra-short-wave receiver," *Proc. Inst. Radio Eng.*, vol. 23, pp. 841–884, Aug. 1935.
[3] F. W. Frink, "The basic principles of super-regenerative reception," *Proc. Inst. Radio Eng.*, vol. 26, pp. 76–106, Jan. 1938.
[4] R. Feick and O. Rojas, "Modeling and simulation of the superregenerative receiver," *IEEE Trans. Consumer Electron.*, vol. 43, pp. 92–102, May 1997.
[5] N. B. Buchanan, V. F. Fusco, and J. A. C. Stewart, "A K_α band super regenerative detector," in *Proc. IEEE MTT-S Int. Microwave Symp. Dig.*, Boston, MA, June 2000, pp. 1585–1588.
[6] N. B. Buchanan, R. Davies, and J. A. C. Stewart, "MMIC K_α band oscillator," *Electron. Lett.*, vol. 32, no. 4, pp. 354–355, Feb. 1996.
[7] W. J. Cunningham, *Introduction to Nonlinear Analysis*. New York: McGraw-Hill, 1958, pp. 301–320.

An Improved Prediction of Series Resistance in Spiral Inductor Modeling With Eddy-Current Effect

Ban-Leong Ooi, Dao-Xian Xu, Pang-Shyan Kooi, and Fu-Jiang Lin

***Abstract*—Based on Kuhn's earlier study on current crowding, an improved expression incorporating the skin effect for the prediction of series resistance in spiral inductor modeling has been derived. A modified model for the spiral inductor, which accounts for the eddy-current effect, is thus proposed. Relatively good agreements between the measured data and the results generated from the model are obtained.**

***Index Terms*—Deembedding, eddy current, quality factor, series resistance, skin effect, spiral inductor.**

I. Introduction

The eddy current, which has a significant effect on the inductance of a monolithic-microwave integrated-circuit (MMIC) spiral inductor, manifests itself not only as skin effect, but also as a proximity effect. At around 1 GHz, it is demonstrated in [1] that the proximity effect between the turns of a MMIC spiral inductor (normally on the cross section of the inductor where the width of the metallic trace is relatively much larger than the thickness) that are in the same plane can be neglected. For frequency below 2 GHz, the skin effect is relatively small in most instances since the metallic trace thickness is typically less than or equal to the skin depth. For frequency above 2 GHz, the resistance increases as the skin effect becomes more prominent [2]. In general, all these effects should be included in the inductor circuit modeling. However, to date, this major current crowding mechanism is missing in the conventional inductor equivalent-circuit modeling [3]–[7]. The

Manuscript received July 31, 2001. This work was supported by the Defence Science Organization National Laboratories, Singapore.

The authors are with the Department of Electrical and Computer Engineering, The National University of Singapore, Singapore.

Publisher Item Identifier 10.1109/TMTT.2002.802337.